Featured in Physics

Material Size Dependence on Fundamental Constants

Lukáš F. Pašteka,[1,2,3,*] Yongliang Hao,[4] Anastasia Borschevsky,[4] Victor V. Flambaum,[5,2] and Peter Schwerdtfeger[2,3]
[1]Department of Physical and Theoretical Chemistry & Laboratory for Advanced Materials, Faculty of Natural Sciences, Comenius University, Mlynská dolina, 84104 Bratislava, Slovakia
[2]Centre for Theoretical Chemistry and Physics, The New Zealand Institute for Advanced Study, Massey University Auckland, Private Bag 102904, 0745 Auckland, New Zealand
[3]Centre for Advanced Study at the Norwegian Academy of Science and Letters, Drammensveien 78, NO-0271 Oslo, Norway
[4]Van Swinderen Institute for Particle Physics and Gravity, University of Groningen, Nijenborgh 4, 9747 AG Groningen, The Netherlands
[5]School of Physics, University of New South Wales, Sydney 2052, Australia

(Received 11 September 2018; revised manuscript received 8 March 2019; published 24 April 2019)

Precise experimental setups for detection of variation of fundamental constants, scalar dark matter, or gravitational waves, such as laser interferometers, optical cavities, and resonant-mass detectors, are directly linked to measuring changes in material size. Here we present calculated and experiment-derived estimates for both α and μ dependence of lattice constants and bond lengths of selected solid-state materials and diatomic molecules that are needed for interpretation of such experiments.

DOI: 10.1103/PhysRevLett.122.160801

Several unification theories and standard model (SM) extensions predict variation of fundamental constants (VFCs) in space and in time [1,2]. It has also been hypothesized that interaction of ordinary matter with a massive scalar dark matter (DM) field can produce slow temporal drifts or oscillations in the values of the fundamental constants [3–5], whereas topological defects in the dark matter field can produce transient VFC [6,7]. The first transient DM detection limits were recently discussed by Wcisło *et al.* [8]. A possible route to observe such drifts or transient effects is through systematic measurements of transitions in atomic and molecular spectra that are sensitive to the variation of dimensionless fundamental quantities such as the fine structure constant $\alpha = e^2/\hbar c$ or the proton-to-electron mass ratio $\mu = m_p/m_e$ [9–14].

Laser interferometers now reach precision far exceeding that of any spectroscopic apparatus and thus offer a new promising direction in the search for VFC [15]. This line of research is directly connected to the dependence of material size on VFC, through the use of resonant-mass detectors [16–19] or cryogenic sapphire and silicon oscillators [20–24]. In order to interpret such experiments, knowledge of dependence of the crystal size on the fundamental constants is needed.

Theoretical investigations of size dependence of molecules and bulk materials on fundamental constants are scarce. Some studies were carried out in the context of relativistic effects and corresponding changes in periodic trends, where the dependence on the fine structure constant is considered [25,26]. More recently, King *et al.* investigated the dependence of structure and bonding in small molecules on both α and μ, with the objective of finding the hypothetical (α, μ) regimes that support biochemistry and therefore life on our planet [27]. Braxmaier *et al.* [28] performed an investigation of the variation of the resonance frequencies of monolithic crystal cavities with possible variation of fundamental constants through the dependence of the refractive index of the medium on α and μ. To the best of our knowledge, no prior investigations of direct size dependence of bulk materials on fundamental constants have been carried out.

In nonrelativistic physics, the size of molecules and solids is proportional to the Bohr radius a_B. This dependence cancels out in the ratio of the sizes. The individual dependence of different compounds on the fine structure constant is determined by the difference in the relativistic effects, which are proportional to $Z^2\alpha^2$ (and higher powers of $Z^2\alpha^2$). Thus, considering the ratio of the resonance frequencies in two optical cavities made from different materials, in the nonrelativistic approximation there is no dependence on α, but such dependence appears due to relativistic corrections.

The situation is different when we compare the resonance frequency of an optical cavity with an atomic optical frequency. For example, one measures the ratio of the Sr atomic clock frequency and the resonance frequency in a silicone cavity of length L [8]. Here, the ratio is proportional to α already in the nonrelativistic approximation because the resonator frequency depends on the speed of light c. Indeed, the resonator frequency is $\omega_r = ck \sim c/\lambda \sim c/L \sim c/a_B$, atomic frequency $\omega_a \sim e^2/\hbar a_B$; therefore, $\omega_a/\omega_r \sim e^2/\hbar c = \alpha$. In this case, relativistic corrections produce additional α dependence.

Another dimensionless ratio that affects the properties of different compounds is the ratio of nuclear and electron masses; the nuclear mass is approximately proportional to

TABLE I. Experimental and calculated bond lengths R_e and their corresponding calculated fractional variation with varying fine-structure constant α and proton-to-electron mass ratio μ.

Mol.	State	R_e [Å]			$(dR_e/R_e)/(d\alpha/\alpha)$		$(dR_0/R_0)/(d\mu/\mu)$	$(dR_e/R_e)/(d\mu/\mu)$
		Exp.[a]	CC	DFT	CC	DFT	Eq. (3)	DBOC-CC
Cu_2	$^1\Sigma_g^+$	2.2197(1)	2.216	2.215	-3.19×10^{-2}	-3.18×10^{-2}	-7.15×10^{-4}	-7.31×10^{-6}
Ag_2	$^1\Sigma_g^+$	2.5303(2)	2.522	2.565	-7.66×10^{-2}	-8.21×10^{-2}	-5.34×10^{-4}	-3.38×10^{-6}
Au_2	$^1\Sigma_g^+$	2.4719(1)	2.471	2.501	-3.15×10^{-1}	-3.37×10^{-1}	-2.95×10^{-4}	9.16×10^{-7}
C_2	$^1\Sigma_g^+$	1.24253(2)	1.243	1.254	-2.65×10^{-4}	-3.88×10^{-4}	-1.17×10^{-3}	-6.94×10^{-6}
Si_2	$^3\Sigma_g^-$	2.246	2.255	2.309	8.66×10^{-5}	1.94×10^{-4}	-7.08×10^{-4}	-6.63×10^{-6}
Ge_2	$^3\Sigma_g^-$	2.3667(6)[b]	2.361	2.430	-6.74×10^{-3}	-6.48×10^{-3}	-4.37×10^{-4}	-4.46×10^{-6}
Sn_2	0_g^+	2.746(1)	2.722	2.814	-2.24×10^{-2}	-2.17×10^{-2}	-3.25×10^{-4}	-3.82×10^{-6}
Pb_2	0_g^+	2.9271(2)	2.869	2.960	-1.05×10^{-1}	-1.58×10^{-1}	-3.37×10^{-4}	3.32×10^{-7}

[a]Experimental values from Refs. [47–52].
[b]For Ge_2, only R_0 was available experimentally. This was used together with the experimental B_0 and α_e value of 2.84×10^{-4} cm^{-1} from our CC calculations to calculate R_e.

the proton mass, and thus we consider the proton-to-electron mass ratio μ.

In this Letter, we present a systematic investigation of the variation of crystal lattice parameters (a_e and c_e) and molecular bond lengths (R_e) due to variation of the fine structure constant and the proton-to-electron mass ratio for selected solid state and molecular systems.

For our solid-state study, we have selected several elemental and compound crystals. The choice of Cu, Si, Al, Nb, and Al_2O_3 was motivated by highly precise experimental setups measuring effects of physics beyond the SM: silicon and sapphire oscillators [20–24] and resonance of Cu, Al, and Nb bars [16–18]. In order to illustrate periodic trends, we have also chosen to study the group 11 and 14 elemental solids.

However, we initially investigated the dependence of the equilibrium interatomic distance R_e of diatomic molecules on α and μ. This gave us the opportunity to test the methodology used for the investigation of solids. For molecules, we have the option of using high-level *ab initio* methodology such as relativistic coupled cluster (CC) theory as a benchmark to our density functional theory (DFT) results. For this part of the study, we chose dimers of group 11 and group 14 elements.

The results of our investigation of diatomic molecules are collected in Table I (see the Supplemental Material [29] for computational details [30–46]). Both CC and DFT calculated equilibrium bond lengths R_e agree with experiment. The mean absolute symmetric percentage error (MASPE) of CC results with respect to experiment is 0.5%. Correspondingly for DFT, the MASPE is 1.6%. Comparing the two methods to one another, we obtain the MASPE value of 1.9%; i.e., DFT recovers the more rigorous CC results very well. In case of the derivative property, the α variation of bond lengths, there are no experimental results. However, comparing the DFT to CC results gives the MASPE of 22%, which we use to evaluate the uncertainty on the predicted DFT α variation of lattice parameters presented below.

Generally, the magnitude of the α dependence on R_e increases with increasing atomic number Z, as one expects. In group 11 (Cu, Ag, Au), the effect follows the well-known $\sim Z^2$ dependence as is the case with many other properties [53]. For group 14 elements (C, Si, Ge, Sn, Pb), we observe a nonmonotonous trend; however, for the heavier elements we still notice an increasing α-sensitivity. This is not surprising, as we note the changes in the ground-state electronic structure in the group 14 element sequence.

The main source of the mass dependence of molecular bond lengths comes from the vibrational motion. Assuming that the rotational constant and bond length relationship is $B \sim R^{-2}$, and the vibrationally averaged rotational constant is

$$B_0 = B_e - \frac{\alpha_e}{2}, \tag{1}$$

where B_e is the equilibrium rotational constant and α_e is the vibrational-rotational coupling constant, we can express the vibrationally averaged bond length R_0 as

$$R_0 = R_e\sqrt{1+\frac{\alpha_e}{2B_e-\alpha_e}}. \tag{2}$$

Following the scaling of equilibrium constants with reduced mass M, $B_e \sim M^{-1}$, and $\alpha_e \sim M^{-\frac{3}{2}}$ [54], we arrive at the fractional variation of R_0 with varying μ

$$\frac{dR_0}{R_0} = -\frac{\alpha_e}{4(2B_e-\alpha_e)}\frac{d\mu}{\mu}. \tag{3}$$

This simple but useful estimate can be evaluated using readily available experimental spectroscopic constants [47–52]. Resulting values are shown in Table I. Because of the negative sign in Eq. (3) and the fact that $\alpha_e \ll B_e$ in all realistic diatomics, these are always negative. The magnitude of the effect is relatively uniform in all investigated systems. Following the Pekeris formula [55] derived for the Morse potential

$$\alpha_e = \frac{6B_e^2}{\omega_e}\left(\sqrt{\frac{\omega_e x_e}{B_e}} - 1\right), \tag{4}$$

we can expect larger fractional variation of R_0 with μ for shallow or strongly anharmonic interatomic potentials.

A small contribution to bond length mass dependence arises from the nuclear kinetic energy terms which are neglected in the Born-Oppenheimer approximation (BOA). Within the BOA, the nuclear motion is separated from the electronic motion, and coupling terms are in practice completely neglected. As a consequence, equilibrium bond lengths are independent of the mass and this near mass invariance is widely used in the experimental determination of bond lengths from rotational spectra of different isotopologues of the same molecule. Taking the nuclear kinetic energy term into account the R_e is in fact weakly linearly dependent on the inverse reduced mass of the molecule [56]. This directly translates into the μ-dependence $R_e \sim \mu^{-1}$.

To estimate the non-BOA contribution to μ sensitivity of bond lengths, we included the perturbative diagonal Born-Oppenheimer corrections (DBOC) in optimizations of the investigated molecules [29]. Results for the μ sensitivity of the fractional variation of R_e are collected in Table I. Generally, the size of this effect is comparable in all investigated diatomics. This contribution is at least 2 orders of magnitude smaller than the fractional variation of R_0 in all cases, and therefore it can be safely neglected when considering the μ sensitivity of vibrationally averaged bond lengths. One can expect this conclusion to be even more justified in solids, where the atoms are further confined by the lattice. We note Lutz and Hutson investigated the role of DBOC in other aspects of diatomic spectroscopy and ultracold physics [57].

We estimate our μ-sensitivity results to be accurate within $\pm 5\%$, considering error bars from experimental determination of spectroscopic parameters and errors introduced by neglecting the higher-order spectroscopic constants (γ_e, ϵ_e, etc.) and the non-BOA effects. The error in α_e determination dominates the resulting compound error of the μ sensitivity.

The investigation of the α and μ sensitivity of lattice parameters of solids was conceptually analogous to the initial study on diatomics [29]. The results of our DFT solid-state calculations are collected in Table II. The calculated equilibrium lattice parameters are in a very good agreement with experimental values, giving the MASPE value of 1.3%, which is slightly smaller than in the case of diatomic molecules. Relying on the error analysis of diatomics, we thus expect the calculated α dependence of lattice constants to be accurate within $\pm 20\%$. Figure 1 demonstrates that the lattice parameters exhibit close to ideal α^2 scaling; i.e., their dependence on x is almost perfectly linear across a wide range of α values (in

TABLE II. Experimental and calculated lattice constants a_e and c_e (c_e shown in the second line for the respective structure) and their corresponding calculated fractional variation with varying fine-structure constant α and proton-to-electron mass ratio μ.

Solid	Structure	Spc. group	a_e, c_e [Å] Exp. (RT)[a]	Exp. (0K)[b]	Calc.	$(da_e/a_e)/(d\alpha/\alpha)$	$(da_0/a_0)/(d\mu/\mu)$
Cu	Fcc	$Fm\bar{3}m$	3.6146(2)	3.6029(2)	3.634	-1.97×10^{-2}	-1.12×10^{-3}
Ag	Fcc	$Fm\bar{3}m$	4.0857(2)	4.0681(2)	4.160	-4.97×10^{-2}	-8.32×10^{-4}
Au	Fcc	$Fm\bar{3}m$	4.0782(2)	4.0646(2)	4.059	-1.61×10^{-1}	-4.33×10^{-4}
C	Dia.	$Fd\bar{3}m$	3.5669(2)	3.5667(2)	3.576	-2.39×10^{-4}	-2.22×10^{-3}
Si	Dia.	$Fd\bar{3}m$	5.4306(2)	5.4259(2)	5.479	-2.17×10^{-4}	-8.56×10^{-4}
Ge	Dia.	$Fd\bar{3}m$	5.6574(2)	5.6487(2)	5.779	6.21×10^{-4}	-6.02×10^{-4}
Sn	Dia. (α)	$Fd\bar{3}m$	6.4892(2)	6.4752(2)	6.678	-4.46×10^{-4}	-3.29×10^{-4}
	Tet. (β)	$I4_1/amd$	5.8318(2)	5.8048(2)	5.956	7.61×10^{-3}	-7.09×10^{-4}
			3.1818(2)	3.1671(2)	3.251	1.16×10^{-3}	
Pb	Fcc	$Fm\bar{3}m$	4.9502(2)	4.9142(2)	4.715	-2.94×10^{-1}	-5.65×10^{-4}
Al	Fcc	$Fm\bar{3}m$	4.0496(2)	4.0321(2)	4.042	3.65×10^{-4}	-2.11×10^{-3}
Nb	Bcc	$Im\bar{3}m$	3.3004(2)	3.2955(2)	3.317	-2.35×10^{-3}	-3.74×10^{-4}
Ti	Hcp	$P6_3/mmc$	2.9506(2)	2.9461(2)	2.935	-1.18×10^{-3}	-7.06×10^{-4}
			4.6835(2)	4.6764(2)	4.685	-3.47×10^{-3}	
Al_2O_3	Hex.	$R\bar{3}c$	4.7540(5)	4.7507(5)	4.825	-4.06×10^{-4}	-2.06×10^{-3}
			12.9820(6)	12.9731(6)	13.142	-4.88×10^{-4}	
SiC	3C (β)	$F\bar{4}3m$	4.3596(1)	4.3582(1)	4.392	-3.54×10^{-4}	-1.56×10^{-3}
	6H (α)	$P6_3mc$	3.0806(1)	3.0795(1)	3.105	-3.73×10^{-4}	-1.47×10^{-3}
			15.1173(1)	15.1121(1)	15.225	-3.41×10^{-4}	
WC	Hex.	$P\bar{6}m2$	2.9059(1)	2.9051(1)	2.923	-4.39×10^{-2}	-1.26×10^{-3}
			2.8377(1)	2.8369(1)	2.857	-3.19×10^{-2}	

[a]Experimental values from Refs. [58–61].
[b]Finite-temperature experimental lattice parameters extrapolated to 0K [62] using experimental data from Refs. [60,61,63–71].

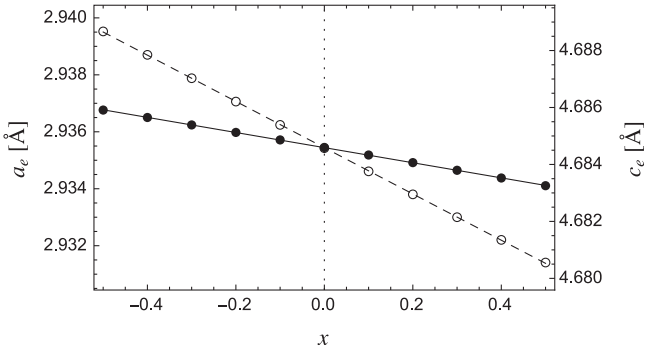

FIG. 1. Dependence of the lattice constants a_e, c_e (full and open circles, respectively) of bulk Ti on the relativistic parameter x. Slopes are shown to scale.

the present study, $\sqrt{0.5}\alpha_0 \leq \alpha \leq \sqrt{1.5}\alpha_0$). We note that the values of fractional variation $(da_e/a_e)/(d\alpha/\alpha)$ are relatively small ($\ll 1$).

We once more observe the general increase of the α sensitivity with Z. In the case of group 11 elements, this increase follows the $\sim Z^2$ scaling (Fig. 2). For group 14, the overall effect is highly nonmonotonic. This is also true if we only compare crystal structures with the same space group $Fd\bar{3}m$ (C, Si, Ge, α-Sn), because the bonding character changes significantly along this sequence from strongly covalent to semimetallic [72]. Another interesting feature is that the α sensitivity of diamond, the lightest element in the group, is larger than expected from the simple scaling law, and larger than that of its heavier homologue, Si. Comparing the two allotropes of tin, we observe opposite sign of the size dependence on α. Furthermore, the absolute α sensitivity of β-Sn is higher than that of α-Sn. This can be ascribed to relativistic effects more strongly influencing the distorted-close-pack structure of β-Sn, which has higher s character compared to fully sp^3-hybridized diamond structure of α-Sn [73]. Relativistic effects are strongest in s orbitals with the highest density in the vicinity of the nucleus. Population analysis gives $5s$:1.54e, $5p$:2.34e for α-Sn and $5s$:1.73e, $5p$:2.14e for β-Sn, supporting this interpretation. For the noncubic

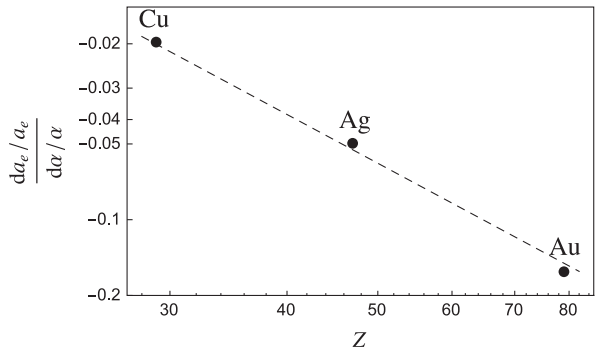

FIG. 2. Z scaling of $(da_e/a_e)/(d\alpha/\alpha)$ for group 11 elements (note the log-log scale). Dashed line shows the ideal Z^2 fit.

crystal structures (corundum, β-tin, α-SiC, WC), we see different α dependence of the lattice constants a_e and c_e, especially in the case of β-Sn, where the α sensitivity of a_e is roughly 6× larger than that of c_e. Thus, the character of bonding has a very strong influence on the dependence of the crystal structure parameters on α, and in the general case scaling laws are not sufficient to estimate the size of the effect.

A general practice for removing the dependence on the unit system is to use the ratio of two observed quantities instead of measuring a property of a single system. In this case, we can either compare two different materials (preferably with opposite signs of their α dependencies, to enhance the sensitivity) or even compare the α sensitivity in two different directions of a single material (for noncubic crystals). Additionally, in interferometry, the observed quantity is the phase shift, which is unitless in itself, and one type of measurement would suffice for topological DM detection.

The mass dependence of lattice parameters is due to the vibrational motion of the crystal lattice. It was extensively studied theoretically and experimentally using isotopic substitution. For monoatomic solids at zero temperature (where the mass dependence is largest [74]), London derived an expression for fractional variation of molar volume V with varying isotopic molar mass M [75]

$$\frac{MdV}{VdM} = -\frac{9}{16}\frac{\gamma\kappa}{V}R\Theta_D, \tag{5}$$

where γ is the thermodynamic Grüneisen parameter, κ the compressibility, R the gas constant, and Θ_D the Debye temperature. This translates to a final expression for the μ variation of the lattice constant

$$\frac{da_0}{a_0}\Big/\frac{d\mu}{\mu} = -\frac{3}{16}\frac{\gamma}{BV}k_B\Theta_D, \tag{6}$$

where B is the isothermal bulk modulus, V is atomic volume, and k_B is Boltzmann constant. Because all numbers entering this formula are positive, the resulting values are negative for all realistic crystals. Note, the bulk modulus and hence also the μ variation are assumed to be isotropic.

Results obtained using expression (6) and available experimental parameters [60,61,63–71] are listed in Table II. Considering the errors in experimental determination of solid-state parameters, we estimate the overall presented μ-sensitivity values to be accurate within ±20%. Our μ sensitivity estimates compare well with the results derived from available experimental measurements on diamond, silicon, and germanium (-1.8×10^{-3}, -7.8×10^{-4}, and -5.5×10^{-4}, respectively) [76–78], as well as with results derived from theoretical path-integral Monte Carlo simulations (C: -1.94×10^{-3}; Si: -1.13×10^{-3}; Ge: -6.55×10^{-4}; β-SiC: -1.37×10^{-3})

[79–82]. The MASPE value of our estimates with respect to the referenced results is 15%, supporting our error analysis. Out of the investigated materials, diamond, Al, and Al_2O_3 (i.e., corundum or sapphire) have the highest μ sensitivity. All results lie in a relatively small range spanning 1 order of magnitude. Within this range, however, there are no clear systematic trends.

Precision interferometry can now provide relative sensitivity of parameters such as $\delta L/L$ to VFC beyond that of any other physical apparatus. Combining this with the calculated fractional variation of crystal sizes and the use of silicon, sapphire or other single crystal oscillators or optical cavities offer a new and independent path to testing VFC and search for scalar low-mass dark matter beyond the most stringent limits [15]. For a progress in this field, accurate values for α and μ dependence of lattice constants of solid-state materials are required, which we provide in this Letter.

To illustrate the expected experimental sensitivity to the variation of the fundamental constants, we present an example. Assume that $\delta\alpha/\alpha = 10^{-17}$ yr^{-1} (this value is close to the present best limit on the variation of α [83]). We may compare variation of relative sizes L of two materials with different sensitivity to α variation, for example, Au and Si with $K_\alpha(\mathrm{Au}) = -0.161$ and $K_\alpha(\mathrm{Si}) = -0.000217$, where the sensitivity coefficients $K = (da_e/a_e)/(d\alpha/\alpha)$ are presented in Table II. The relative variation of the ratio of the sizes is then $[\delta(L_{\mathrm{Au}}/L_{\mathrm{Si}})/(L_{\mathrm{Au}}/L_{\mathrm{Si}})] = [K_\alpha(\mathrm{Au}) - K_\alpha(\mathrm{Si})](\delta\alpha/\alpha) = -1.6 \times 10^{-18}$.

This is comparable to the precision of the recent optical cavity experiments [84–86], where the crystal-size variation directly affects the measurement. The highest reported precision for an optical cavity is $5.8(3) \times 10^{-19}$ after an hour of averaging [87]. Longer averaging times may lead to an even higher precision. Therefore, the results presented here support the proposed method as an alternative avenue to test the VFC. Performing a wider search and identifying suitable materials with higher sensitivity coefficients in the future would further improve the prospects of the proposed method.

Currently, the highest instrumental precision is achieved in the large-scale interferometer setups (LIGO, VIRGO), reaching 10^{-22} levels [88]. However, because here the effect of the crystal-size variation is not as direct as for the optical cavities, application of the present method would require some modification of the detection scheme.

As explained in the introduction, the sensitivity coefficient for comparison of a resonator frequency and an atomic clock frequency in the nonrelativistic limit is given by the difference $K_{\mathrm{resonator}} - K_{\mathrm{clock}} = 1$; i.e., the effect is equal to $\delta\alpha/\alpha = 10^{-17}$. To include the relativistic corrections, we should add to the sensitivity coefficients of the resonator the values presented in Table II and for the clock the values presented in Ref. [9]. For the Si optical cavity and Sr clock, the relativistic corrections are not significant; however, for clocks based on heavy elements (such as Hg^+ and Yb^+), relativistic effects increase the sensitivity to $\delta\alpha/\alpha$ several times.

The authors are grateful to J. Ye, P. Wcisło, J. Robinson, M. Kozlov, and D. Budker for fruitful discussions, and to the Mainz Institute for Theoretical Physics for its hospitality and its partial support during the completion of this Letter. The authors would also like to thank the Center for Information Technology of the University of Groningen for providing access to the Peregrine high performance computing cluster and for their technical support. L. F. P. acknowledges the support from the Slovak Research and Development Agency under the Contract No. APVV-15-0105. V. V. F. acknowledges support from the Australian Research Council Grant No. DP150101405

*Corresponding author.
lukas.f.pasteka@uniba.sk

[1] J.-P. Uzan, Varying constants, gravitation and cosmology, Living Rev. Relativity **14**, 2 (2011).
[2] J. D. Barrow, Varying constants, Phil. Trans. R. Soc. A **363**, 2139 (2005).
[3] Y. V. Stadnik and V. V. Flambaum, Can dark matter induce cosmological evolution of the fundamental constants of nature, Phys. Rev. Lett. **115**, 201301 (2015).
[4] Y. V. Stadnik and V. V. Flambaum, Searching for dark matter and variation of fundamental constants with laser and maser interferometry, Phys. Rev. Lett. **114**, 161301 (2015).
[5] A. Arvanitaki, J. Huang, and K. Van Tilburg, Searching for dilaton dark matter with atomic clocks, Phys. Rev. D **91**, 015015 (2015).
[6] A. Derevianko and M. Pospelov, Hunting for topological dark matter with atomic clocks, Nat. Phys. **10**, 933 (2014).
[7] Y. V. Stadnik and V. V. Flambaum, Searching for topological defect dark matter via nongravitational signatures, Phys. Rev. Lett. **113**, 151301 (2014); Stadnik and Flambaum Reply:, Phys. Rev. Lett. **116**, 169002 (2016).
[8] P. Wcisło, P. Morzyński, M. Bober, A. Cygan, D. Lisak, R. Ciuryło, and M. Zawada, Experimental constraint on dark matter detection with optical atomic clocks, Nat. Astron. **1**, 0009 (2016).
[9] V. V. Flambaum and V. A. Dzuba, Search for variation of the fundamental constants in atomic, molecular, and nuclear spectra, Can. J. Phys. **87**, 25 (2009).
[10] C. Chin, V. V. Flambaum, and M. G. Kozlov, Ultracold molecules: New probes on the variation of fundamental constants, New J. Phys. **11**, 055048 (2009).
[11] P. Jansen, H. L. Bethlem, and W. Ubachs, Perspective: Tipping the scales: Search for drifting constants from molecular spectra, J. Chem. Phys. **140**, 010901 (2014).
[12] L. F. Pašteka, A. Borschevsky, V. V. Flambaum, and P. Schwerdtfeger, Search for the variation of fundamental constants: Strong enhancements in $X\ ^2\Pi$ cations of dihalogens and hydrogen halides, Phys. Rev. A **92**, 012103 (2015).
[13] M. G. Kozlov and S. A. Levshakov, Microwave and submillimeter molecular transitions and their dependence on

fundamental constants, Ann. Phys. (Berlin) **525**, 452 (2013).
[14] M. S. Safronova, D. Budker, D. DeMille, D. F. Jackson Kimball, A. Derevianko, and C. W. Clark, Search for new physics with atoms and molecules, Rev. Mod. Phys. **90**, 025008 (2018).
[15] Y. V. Stadnik and V. V. Flambaum, Enhanced effects of variation of the fundamental constants in laser interferometers and application to dark-matter detection, Phys. Rev. A **93**, 063630 (2016).
[16] A. Arvanitaki, S. Dimopoulos, and K. Van Tilburg, Sound of dark matter: Searching for light scalars with resonant-mass detectors, Phys. Rev. Lett. **116**, 031102 (2016).
[17] P. Astone *et al.* (International Gravitational Event Collaboration), Methods and results of the IGEC search for burst gravitational waves in the years 1997–2000, Phys. Rev. D **68**, 022001 (2003).
[18] P. Astone *et al.* (IGEC-2 Collaboration), Results of the IGEC-2 search for gravitational wave bursts during 2005, Phys. Rev. D **76**, 102001 (2007).
[19] O. D. Aguiar, Past, present and future of the resonant-mass gravitational wave detectors, Res. Astron. Astrophys. **11**, 1 (2011).
[20] M. E. Tobar, P. Wolf, S. Bize, G. Santarelli, and V. Flambaum, Testing local Lorentz and position invariance and variation of fundamental constants by searching the derivative of the comparison frequency between a cryogenic sapphire oscillator and hydrogen maser, Phys. Rev. D **81**, 022003 (2010).
[21] J. G. Hartnett, N. R. Nand, and C. Lu, Ultra-low-phase-noise cryocooled microwave dielectric-sapphire-resonator oscillators, Appl. Phys. Lett. **100**, 183501 (2012).
[22] E. Wiens, A. Yu. Nevsky, and S. Schiller, Resonator with ultrahigh length stability as a probe for equivalence-principle-violating physics, Phys. Rev. Lett. **117**, 271102 (2016).
[23] T. Kessler, C. Hagemann, C. Grebing, T. Legero, U. Sterr, F. Riehle, M. J. Martin, L. Chen, and J. Ye, A sub-40-MHz-linewidth laser based on a silicon single-crystal optical cavity, Nat. Photonics **6**, 687 (2012).
[24] E. Wiens, Q.-F. Chen, I. Ernsting, H. Luckmann, U. Rosowski, A. Nevsky, and S. Schiller, Silicon single-crystal cryogenic optical resonator, Opt. Lett. **39**, 3242 (2014); Erratum, Opt. Lett. **40**, 68(E) (2015).
[25] P. Pyykkö, Relativistic effects in structural chemistry, Chem. Rev. **88**, 563 (1988).
[26] T. Söhnel, H. Hermann, and P. Schwerdtfeger, Towards the understanding of solid-state structures: From cubic to chainlike arrangements in group 11 halides, Angew. Chem., Int. Ed. **40**, 4381 (2001).
[27] R. A. King, A. Siddiqi, W. D. Allen, and H. F. Schaefer, Chemistry as a function of the fine-structure constant and the electron-proton mass ratio, Phys. Rev. A **81**, 042523 (2010).
[28] C. Braxmaier, O. Pradl, H. Müller, A. Peters, J. Mlynek, V. Loriette, and S. Schiller, Proposed test of the time independence of the fundamental constants α and m_e/m_p using monolithic resonators, Phys. Rev. D **64**, 042001 (2001).
[29] See Supplemental Material at http://link.aps.org/supplemental/10.1103/PhysRevLett.122.160801 for computational details.
[30] J. P. Perdew, K. Burke, and M. Ernzerhof, Generalized gradient approximation made simple, Phys. Rev. Lett. **77**, 3865 (1996); Erratum, Phys. Rev. Lett. **78**, 1396(E) (1997).
[31] K. G. Dyall, Relativistic double-zeta, triple-zeta, and quadruple-zeta basis sets for the 5d elements Hf–Hg, Theor. Chem. Acc. **112**, 403 (2004).
[32] K. G. Dyall, Relativistic quadruple-zeta and revised triple-zeta and double-zeta basis sets for the 4p, 5p, and 6p elements, Theor. Chem. Acc. **115**, 441 (2006).
[33] K. G. Dyall, Relativistic double-zeta, triple-zeta, and quadruple-zeta basis sets for the 4d elements Y–Cd, Theor. Chem. Acc. **117**, 483 (2007).
[34] DIRAC, a relativistic *ab initio* electronic structure program, Release DIRAC15 (2015); R. Bast *et al.*, http://www.diracprogram.org.
[35] K. Koepernik and H. Eschrig, Full-potential nonorthogonal local-orbital minimum-basis band-structure scheme, Phys. Rev. B **59**, 1743 (1999).
[36] H. Eschrig, M. Richter, and I. Opahle, Relativistic solid state calculations, in *Relativistic Electronic Structure Theory: Part 2. Applications*, Theoretical and Computational Chemistry, Vol. 14, edited by P. Schwerdtfeger (Elsevier, Amsterdam, 2004), pp. 723–776.
[37] The Munich SPR-KKR package, version 6.3; H. Ebert *et al.*, http://ebert.cup.uni-muenchen.de/SPRKKR.
[38] H. Ebert, D. Ködderitzsch, and J. Minár, Calculating condensed matter properties using the KKR-Green's function method—recent developments and applications, Rep. Prog. Phys. **74**, 096501 (2011).
[39] H. Ebert, Fully relativistic band structure calculations for magnetic solids—formalism and application, in *Electronic Structure and Physical Properties of Solids*, Lecture Notes in Physics, Vol. 535 (Springer, Berlin, Heidelberg, 2000), pp. 191–246.
[40] CFOUR, Coupled-cluster techniques for computational chemistry, a quantum-chemical program package by J. F. Stanton, J. Gauss, M. E. Harding, P. G. Szalay with contributions from A. A. Auer *et al.* and the integral packages MOLECULE (J. Almlöf and P. R. Taylor), PROPS (P. R. Taylor), ABACUS (T. Helgaker, H. J. Aa. Jensen, P. Jørgensen, and J. Olsen), and ECP routines by A. V. Mitin and C. van Wüllen. For the current version, see http://www.cfour.de.
[41] J. Gauss, A. Tajti, M. Kállay, J. F. Stanton, and P. G. Szalay, Analytic calculation of the diagonal Born-Oppenheimer correction within configuration-interaction and coupled-cluster theory, J. Chem. Phys. **125**, 144111 (2006).
[42] A. Canal Neto, E. P. Muniz, R. Centoducatte, and F. E. Jorge, Gaussian basis sets for correlated wave functions. Hydrogen, helium, first- and second-row atoms, J. Mol. Struct. **718**, 219 (2005).
[43] G. G. Camiletti, S. F. Machado, and F. E. Jorge, Gaussian basis set of double zeta quality for atoms K through Kr: Application in DFT calculations of molecular properties, J. Comput. Chem. **29**, 2434 (2008).
[44] C. L. Barros, P. J. P. de Oliveira, F. E. Jorge, A. Canal Neto, and M. Campos, Gaussian basis set of double zeta quality for atoms Rb through Xe: Application in non-relativistic and relativistic calculations of atomic and molecular properties, Mol. Phys. **108**, 1965 (2010).

[45] A. Canal Neto and F. E. Jorge, All-electron double zeta basis sets for the most fifth-row atoms: Application in DFT spectroscopic constant calculations, Chem. Phys. Lett. **582**, 158 (2013).

[46] Y. Imafuku, M. Abe, M. W. Schmidt, and M. Hada, Heavy element effects in the diagonal Born-Oppenheimer correction within a relativistic spin-free hamiltonian, J. Phys. Chem. A **120**, 2150 (2016).

[47] K. P. Huber and G. Herzberg, *Constants of Diatomic Molecules*, Molecular Spectra and Molecular Structure, Vol. 4 (Van Nostrand Reinhold, New York, 1979).

[48] V. Beutel, H. G. Krämer, G. L. Bhale, M. Kuhn, K. Weyers, and W. Demtrder, High resolution isotope selective laser spectroscopy of Ag_2 molecules, J. Chem. Phys. **98**, 2699 (1993).

[49] B. Simard and P. A. Hackett, High resolution study of the (0,0) and (1,1) bands of the $A0_u^+ - X0_g^+$ system of Au_2, J. Mol. Spectrosc. **142**, 310 (1990).

[50] D. A. Hostutler, H. Li, D. J. Clouthier, and G. Wannous, Exploring the bermuda triangle of homonuclear diatomic spectroscopy: The electronic spectrum and structure of Ge_2, J. Chem. Phys. **116**, 4135 (2002).

[51] V. E. Bondybey, M. Heaven, and T. A. Miller, Laser vaporization of tin: Spectra and ground state molecular parameters of Sn_2, J. Chem. Phys. **78**, 3593 (1983).

[52] M. C. Heaven, T. A. Miller, and V. E. Bondybey, Laser spectroscopy of lead molecules produced by laser vaporization, J. Phys. Chem. **87**, 2072 (1983).

[53] J. Autschbach, S. Siekierski, M. Seth, P. Schwerdtfeger, and W. H. E. Schwarz, Dependence of relativistic effects on electronic configuration in the neutral atoms of d- and f-block elements, J. Comput. Chem. **23**, 804 (2002).

[54] R. Mulliken, The isotope effect in band spectra, part I, Phys. Rev. **25**, 119 (1925).

[55] C. Pekeris, The rotation-vibration coupling in diatomic molecules, Phys. Rev. **45**, 98 (1934).

[56] J. K. G. Watson, The isotope dependence of the equilibrium rotational constants in $^1\sum$ states of diatomic molecules, J. Mol. Spectrosc. **45**, 99 (1973).

[57] J. J. Lutz and J. M. Hutson, Deviations from Born-Oppenheimer mass scaling in spectroscopy and ultracold molecular physics, J. Mol. Spectrosc. **330**, 43 (2016).

[58] H. W. King, Crystal structures and lattice parameters of allotropes of the elements, in CRC Handbook of Chemistry and Physics, 97th ed., edited by W. M. Haynes (CRC Press, Boca Raton, 2017), Chap. 12, pp. 16–19.

[59] E. N. Maslen, V. A. Streltsov, N. R. Streltsova, N. Ishizawa, and Y. Satow, Synchrotron X-ray study of the electron density in α-Al_2O_3, Acta Crystallogr. Sect. B **49**, 973 (1993).

[60] *Group IV Elements, IV-IV and III-V Compounds. Part b—Electronic, Transport, Optical and Other Properties*, edited by O. Madelung, U. Rössler, and M. Schulz, Landolt-Börnstein—Group III Condensed Matter Vol. 41A1b (Springer-Verlag, Berlin, Heidelberg, 2002).

[61] K. D. Litasov, A. Shatskiy, Y. Fei, A. Suzuki, E. Ohtani, and K. Funakoshi, Pressure-volume-temperature equation of state of tungsten carbide to 32 GPa and 1673 K, J. Appl. Phys. **108**, 053513 (2010).

[62] G. B. Mitra and A. K. Giri, Gruneisen's law and extrapolated values of lattice constants of single-phase copper-aluminium alloys at absolute zero, J. Phys. D **19**, 1065 (1986).

[63] C. Kittel, *Introduction to Solid State Physics*, 8th ed. (Wiley, New York, 2005).

[64] D. C. Wallace, *Statistical Physics of Crystals and Liquids: A Guide to Highly Accurate Equations of State* (World Scientific, Singapore, 2002).

[65] I. V. Aleksandrov, A. F. Goncharov, A. N. Zisman, and S. M. Stishov, Diamond at high pressures: Raman scattering of light, equation of state, and a high pressure scale, J. Exp. Theor. Phys. **66**, 384 (1987).

[66] S. M. Stishov, Energy, compressibility, and covalence in the carbon family, J. Exp. Theor. Phys. Lett. **71**, 15 (2000).

[67] A. F. Goncharov, Diamond stability under high pressure, Sov. Phys. Usp. **30**, 525 (1987).

[68] *Group IV Elements, IV-IV and III-V Compounds. Part a—Lattice Properties*, edited by O. Madelung, U. Rössler, and M. Schulz, Landolt-Börnstein—Group III Condensed Matter Vol. 41A1a (Springer-Verlag, Berlin, Heidelberg, 2001).

[69] J. A. Rayne and B. S. Chandrasekhar, Elastic constants of β tin from 4.2°K to 300°K, Phys. Rev. **120**, 1658 (1960).

[70] L. V. Al'tshuler, A. A. Bakanova, and R. F. Trunin, Shock adiabats and zero isotherms of seven metals at high pressures, J. Exp. Theor. Phys. **15**, 65 (1962).

[71] R. Tarumi, H. Ledbetter, H. Ogi, and M. Hirao, Low-temperature elastic constants of monocrystal corundum (α-Al_2O_3), Philos. Mag. **93**, 4532 (2013).

[72] A. Hermann, J. Furthmüller, H. W. Gäggeler, and P. Schwerdtfeger, Spin-orbit effects in structural and electronic properties for the solid state of the group-14 elements from carbon to superheavy element 114, Phys. Rev. B **82**, 155116 (2010).

[73] F. Legrain and S. Manzhos, Understanding the difference in cohesive energies between alpha and beta tin in DFT calculations, AIP Adv. **6**, 045116 (2016).

[74] P. Pavone and S. Baroni, Dependence of the crystal lattice constant on isotopic composition: Theory and ab initio calculations for C, Si, and Ge, Solid State Commun. **90**, 295 (1994).

[75] H. London, The difference in the molekular volume of isotopes, Z. Phys. Chem. **16**, 302 (1958).

[76] H. Holloway, K. C. Hass, M. A. Tamor, T. R. Anthony, and W. F. Banholzer, Isotopic dependence of the lattice constant of diamond, Phys. Rev. B **44**, 7123 (1991); Erratum, Phys. Rev. B **45**, 6353(E) (1992).

[77] H.-C. Wille, Yu. V. Shvyd'ko, E. Gerdau, M. Lerche, M. Lucht, H. D. Rüter, and J. Zegenhagen, Anomalous isotopic effect on the lattice parameter of silicon, Phys. Rev. Lett. **89**, 285901 (2002).

[78] M. Y. Hu, H. Sinn, A. Alatas, W. Sturhahn, E. E. Alp, H. C. Wille, Yu. V. Shvyd'ko, J. P. Sutter, J. Bandaru, E. E. Haller, V. I. Ozhogin, S. Rodriguez, R. Colella, E. Kartheuser, and M. A. Villeret, Effect of isotopic composition on the lattice parameter of germanium measured by x-ray backscattering, Phys. Rev. B **67**, 113306 (2003).

[79] C. P. Herrero, The isotopic mass and lattice parameter of diamond; a path-integral simulation, J. Phys. Condens. Matter **13**, 5127 (2001).

[80] C. P. Herrero, Dependence of the silicon lattice constant on isotopic mass, Solid State Commun. **110**, 243 (1999).
[81] J. C. Noya, C. P. Herrero, and R. Ramírez, Isotope dependence of the lattice parameter of germanium from path-integral Monte Carlo simulations, Phys. Rev. B **56**, 237 (1997).
[82] C. P. Herrero, R. Ramírez, and M. Cardona, Isotope effects on the lattice parameter of cubic SiC, Phys. Rev. B **79**, 012301 (2009).
[83] A. D. Ludlow, M. M. Boyd, J. Ye, E. Peik, and P. O. Schmidt, Optical atomic clocks, Rev. Mod. Phys. **87**, 637 (2015).
[84] J. M. Robinson, E. Oelker, W. R. Milner, W. Zhang, T. Legero, D. G. Matei, F. Riehle, U. Sterr, and J. Ye, Crystalline optical cavity at 4 K with thermal-noise-limited instability and ultralow drift, Optica **6**, 240 (2019).
[85] W. Zhang, J. M. Robinson, L. Sonderhouse, E. Oelker, C. Benko, J. L. Hall, T. Legero, D. G. Matei, F. Riehle, U. Sterr, and J. Ye, Ultrastable silicon cavity in a continuously operating closed-cycle cryostat at 4 K, Phys. Rev. Lett. **119**, 243601 (2017).
[86] D. G. Matei, T. Legero, S. Häfner, C. Grebing, R. Weyrich, W. Zhang, L. Sonderhouse, J. M. Robinson, J. Ye, F. Riehle, and U. Sterr, 1.5 μm Lasers with sub-10 MHz linewidth, Phys. Rev. Lett. **118**, 263202 (2017).
[87] E. Oelker, R. B. Hutson, C. J. Kennedy, L. Sonderhouse, T. Bothwell, A. Goban, D. Kedar, C. Sanner, J. M. Robinson, G. E. Marti, D. G. Matei, T. Legero, M. Giunta, R. Holzwarth, F. Riehle, U. Sterr, and J. Ye, Optical clock intercomparison with 6×10^{-19} precision in one hour, arXiv:1902.02741.
[88] J. Aasi *et al.* (LIGO Scientific Collaboration), Advanced LIGO, Classical Quantum Gravity **32**, 115012 (2015).